Acta Cryst. (1977). B33, 2496–2501

Long-Period Stacking Variants and their Electron-Concentration Dependence in the Mg-Base Friauf–Laves Phases

BY Y. KOMURA AND Y. KITANO

Faculty of Science, Hiroshima University, Higashi-senda-machi, Hiroshima 730, *Japan*

(*Received* 2 *December* 1976; *accepted* 3 *February* 1977)

Three new stacking variants have been found in the systems $MgZn_2$–$MgAg_2$ and $MgCu_2$–$MgAl_2$. The crystal structure of $Mg(Zn_{0.90}Ag_{0.10})_2$ has been determined by X-ray diffraction methods. The structure is a rhombohedral 21*R*, *ABC'B'ABC'BCA'C'BCA'CAB'A'CAB'*, consisting of six fundamental composite layers of the Friauf–Laves phases. The space group is $R\bar{3}m$, with 42 formula units in a hexagonal unit cell of dimensions $a = 5{\cdot}21$, $c = 90{\cdot}3$ Å. Two stacking variants in specimens of $Mg(Cu_{0.535}Al_{0.465})_2$ have been analysed by electron diffraction methods. The structures are 6*H*, *ABC'B'AB'*, and 16*H*, *ABC'BCA'CAB'A'CA'C'BC'B'*. Their respective space groups are $P\bar{6}m2$ with 12 formula units in a unit cell with $a = 5{\cdot}14$, $c = 25{\cdot}3$ Å, and $P6_3/mmc$ with 32 formula units in a cell with $a = 5{\cdot}14$, $c = 67{\cdot}4$ Å. A series of structures hitherto found in the Mg-base Friauf–Laves phases is given in order of increasing electron concentration. Then, the fraction of the *h* sequence in the series decreases in the range of $e/a = 0{\cdot}67$–$1{\cdot}33$, but increases in the range of $1{\cdot}33$–$2{\cdot}00$ in order. The newly found structures are included in proper positions in the series. The close relation between electron concentration and the stabilization of stacking variants has thus been confirmed.

Introduction

Friauf–Laves phases are generally considered as size-factor compounds. However, the electronic factor is of great importance in the stabilization of various stacking variants observed in many Mg-base ternary phases. Laves & Witte (1936) investigated alloys of Mg-base Friauf–Laves phases and found that, for instance, the replacement of Cu in $MgCu_2$ by a metal of higher valency, such as Zn, Al or Si, resulted in the change of the cubic $C_{15}(MgCu_2)$ type into the hexagonal $C_{14}(MgZn_2)$ or $C_{36}(MgNi_2)$, depending on the electron concentration (e/a). Lieser & Witte (1952) studied the pseudobinary systems $MgCu_2$–$MgZn_2$, $MgZn_2$–$MgNi_2$ and $MgCu_2$–$MgNi_2$, and found a close relation between electron concentration and crystal structure, *i.e.* the phase boundaries of C_{14}, C_{15} and C_{36} appear at nearly the same values of e/a for all the systems under consideration. Komura, Mitarai, Nakatani, Iba & Shimizu (1970) and Komura, Mitarai, Nakaue & Tsujimoto (1972) reinvestigated the pseudobinary systems $MgZn_2$–$MgCu_2$, $MgCu_2$–$MgNi_2$, $MgZn_2$–$MgNi_2$ and $MgZn_2$–$MgAg_2$ in detail, and ascertained that the crystal structures of these systems are strongly governed by the electron concentration. In addition, four stacking variants were found between the homogeneity ranges of C_{14}, C_{15} and C_{36}-type structures. The four stacking variants are 6, 8, 9 and 10-layer type structures in terms of their layer stacking. Kripyakevich & Melnyk (1974) also reported the effect of electron concentration on the crystal structure for the system $MgZn_2$–$MgLi_2$ which includes stacking variants of 8, 9, 10 and also 14-layer type structures. In the system $MgCu_2$–$MgAl_2$, on the other hand, the structural change has not been well established, though a few stacking variants have been found accompanying many stacking faults in the alloy specimens (Komura, 1962).*

Electron-microscope observation of the Friauf–Laves phase was carried out for the first time by Allen, Delavignette & Amelinckx (1972), and they observed lattice images and crystal defects in $TiCr_2$ and $TiCo_2$. Three stacking variants of 4, 6, and 12-layer types were found in these alloys besides 2 and 3-layer type structures.

In a recent experiment two new stacking variants of 6 and 16-layer types were recognized in the $MgCu_2$–$MgAl_2$ system by means of electron diffraction and lattice images by Kitano, Komura & Kajiwara (1977). We reinvestigated the pseudobinary systems $MgZn_2$–$MgAg_2$ in the complicated range of $e/a = 1{\cdot}90 \sim 2{\cdot}00$, and found a new long-period stacking variant of 21-layer type. The purpose of the present paper is to report the crystal structures of the newly found 6, 16 and 21-layer type stacking variants and to discuss the dependence of the structural changes on the electron concentration, including the new stacking variants, in connexion with the fraction of the hexagonal sequence. A summary of the stacking variants hitherto found in

* In the paper stacking variants of 9-layer and 5-layer types were reported. However, the existence of the 5-layer structure is in doubt, it may be a 10-layer type structure with stacking faults. In fact a 10-layer type structure was found in this alloy system (Kitano, Komura & Kajiwara, 1977). The structure is isostructural with the one already determined (Komura, Kishida & Inoue, 1967), contrary to the disordered stacking of the 5-layer structures.

the Mg-base Friauf–Laves phase is given, which confirms the close relation between electron concentration and the stabilization of stacking variants.

Experimental

Alloys were prepared by melting together pure Mg, Cu and Cu–Al mother alloy for the system $MgCu_2$–$MgAl_2$, and Mg, Zn and Ag metals for the system $MgZn_2$–$MgAg_2$ in an argon-filled induction furnace. All materials used were above 99·9% grade purity. The melt was vigorously stirred and then cast into a cylindrical graphite mould. Alloys obtained were then annealed at various temperatures between 400 and 700 °C in a small graphite crucible placed inside an argon-filled sealed silica tube. Nominal compositions of the specimens were $MgCu_2$–46·5%$MgAl_2$ and $MgZn_2$–10·0%$MgAg_2$, which correspond to e/a = 1·95 and 1·93, respectively. Chemical analysis has not yet been done. After identifying the phases by X-ray powder diffraction, single crystals for X-ray work were obtained by picking out tiny fragments with a linear dimension of about 50 μm from crushed ingots. Precession and Weissenberg photographs were taken with Cu $K\alpha$ radiation. Intensities of reflexions were estimated visually by comparison with a calibrated intensity scale.

A part of an ingot of $MgCu_2$–$MgAl_2$ was sliced into discs 0·2 mm thick which were electrolytically polished in a mixed solution of HNO_3 and CH_3OH. They were used for the electron diffraction and lattice imaging study in a JEM 200A electron microscope at an accelerating voltage of 200 kV. The intensities of the electron diffraction patterns were estimated visually and also by means of a microphotometer, and they were compared with the calculated intensities of possible structure models.

Results

Structure of new stacking variants

The structures of Friauf–Laves phases and their stacking variants can be described in terms of the stacking sequence of six kinds of compound layers (Komura, 1962). These six layers are called A, A', B, B', C and C', each of which is composed of a kagomé net and three triangular nets. The two layers called A and A' are shown in Fig. 1 as examples. If A and A' are shifted by $\frac{1}{3}$ or $\frac{2}{3}$ in the $[\bar{1}10]$ direction of the hexagonal cell, one obtains B and B', or C and C' layers respectively. The possible ways of stacking the layers are shown in Fig. 2. If we continue to stack the layers of A, B, C only or A', B', C' only, we obtain the cubic 3-layer type structure (C_{15}) $ABCABC\ldots$ or $A'C'B'A'C'B'\ldots$

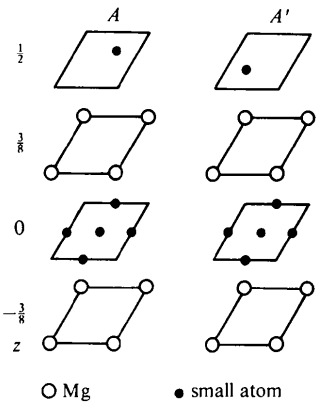

Fig. 1. Two compound layers A and A' of the Friauf–Laves phase. The parameter z is taken as a fraction of the distance between two kagomé nets.

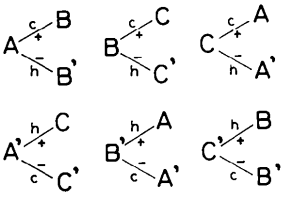

Fig. 2. Possible ways of stacking the six compound layers. Layer sequence symbols c, h and positive and negative changes +, − are also inserted.

On the other hand, the hexagonal 2-layer type structure (C_{14}) can be represented as $AB'AB'\ldots$, $BC'BC'\ldots$ or $CA'CA'\ldots$ Such stackings as $A \rightarrow B$, $B \rightarrow C$, $C \rightarrow A$, $A' \rightarrow C'$, $C' \rightarrow B'$ and $B' \rightarrow A'$ can be called a c sequence, and the other stackings such as $A \rightarrow B'$, $B \rightarrow C'$, $C \rightarrow A'$, $A' \rightarrow C$, $B' \rightarrow A$ and $C' \rightarrow B$ an h sequence. As pointed out in a previous paper (Komura, Kishida & Inoue, 1967) the layer stackings of $A \rightarrow B \rightarrow C \rightarrow A$ and $A' \rightarrow C' \rightarrow B' \rightarrow A'$ in the Laves phase can be called positive (+) and negative (−) changes, respectively, in Zhdanov (1945) symbols. These symbols are also inserted in Fig. 2.

*Rhombohedral 21R**

In the precession and Weissenberg photographs of $MgZn_2$–10% $MgAg_2$ there were several single crystals which showed a periodicity of 21 layers stacked in a rhombohedral fashion. Photographs often showed a coalescence of 4H and 21R structures. There are only five models which satisfy the 21-layer type rhombohedral structure. Every model is characterized by a sequence of numbers, each of which represents the number of successions of positive and negative changes. The total number of positive and negative changes is expressed by 7 × 3 = 21. The five models are as follows:

* Symbols nH, nR represent stacking variants following Ramsdell's (1947) notation.

(1) $ABCABCA'CABCABC'BCABCAB'$ $(6\bar{1})_3$
(2) $ABCAB'A'C'BCABC'B'A'CABCA'C'B'$ $(4\bar{3})_3$
(3) $ABCA'C'BC'BCAB'A'CA'CABC'B'AB'$ $(3\bar{2}1\bar{1})_3$
(4) $ABC'B'ABC'BCA'C'BCA'CAB'A'CAB'$ $(2221)_3$
(5) $ABC'BC'BC'BCA'CA'CA'CAB'AB'AB'$ $(2\bar{1}1\bar{1}1\bar{1})_3$.

Referring to Fig. 1, the layer form factors of A, A', B, B', C and C' are given by

$$V_A = 2f_a \cos\tfrac{3}{8}\varphi + f_b[(-1)^h + (-1)^k + (-1)^{h-k}] + f_b\varepsilon \exp\left(i\frac{\varphi}{2}\right), \quad (1)$$

$$V_A' = 2f_a \cos\tfrac{3}{8}\varphi + f_b[(-1)^h + (-1)^k + (-1)^{h-k}] + f_b\varepsilon^* \exp\left(i\frac{\varphi}{2}\right), \quad (2)$$

$$V_B = V_A\varepsilon^*, \quad V_{B'} = V_{A'}\varepsilon^*, V_C = V_A\varepsilon, V_{C'} = V_{A'}\varepsilon, \quad (3)$$

where $\varepsilon = \exp[2\pi i(h-k)/3]$, and φ is the phase shift due to one layer, which is equal to $2\pi l/21$ in this case. Here f_a is the atomic scattering factor for Mg and f_b that for the other atoms (Zn or Ag). The structure factor of $20l$ reflexions of a given 21-layer model can be calculated on the basis of the following expression:

$$F_{\text{cal}}(20l) = \sum_{m=0}^{20} V_m \exp(im\varphi), \quad (4)$$

where V_m represents the layer form factor of the mth layer [equation (1), (2) or (3)]. In Fig. 3 the observed structure factors of $20l$ reflexions are compared with those calculated for the five models, from $l = 1$ to 46 for every third index. From Fig. 3 it can be easily concluded that the correct layer sequence is No. 4, $ABC'B'ABC'BCA'C'BCA'CAB'A'CAB'$. The space group is $R\bar{3}m$ with 42 formula units of $Mg(Zn_{0.90}Ag_{0.10})_2$ in a hexagonal unit cell of dimensions a = 5·21, c = 90·3 Å. The positional parameters thus obtained in the hexagonal cell are listed in Table 1, where the origin of the above sequence (No. 4) is shifted by 17/21 in the **c** direction. The 126 atoms are placed in the 15 different positions, and Zn and Ag atoms are assumed to be distributed at random in proportion to their composition.

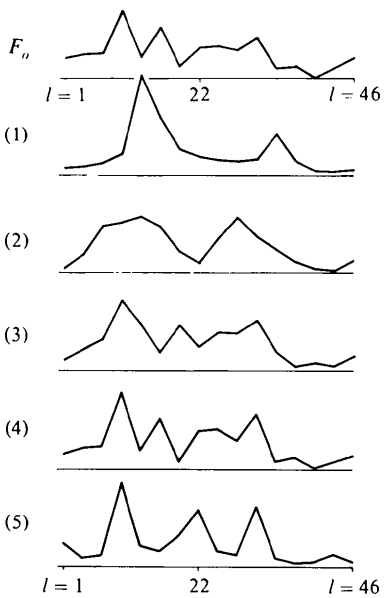

Fig. 3. Comparison of the observed (F_o) and calculated structure factors of $20l$ reflexions for five models of $21R$. (1) $(6\bar{1})_3$, (2) $(4\bar{3})_3$, (3) $(3\bar{2}1\bar{1})_3$, (4) $(2\bar{2}2\bar{1})_3$, (5) $(2\bar{1}1\bar{1}1\bar{1})_3$.

Hexagonal 6H and 16H

Electron-microscope observation revealed two new stacking variants of $6H$ and $16H$ structures in the system $MgCu_2$–46·5% $MgAl_2$. Although the intensities of the diffracted electrons are affected by multiple diffraction, the intensity distributions of the new

Table 1. *Atomic parameters of the 21R structure with space group $R\bar{3}m$*

	Positions	x	y	z
Mg(1)	6(*c*)	0	0	1/56
Mg(2)	6(*c*)	0	0	13/168
Mg(3)	6(*c*)	0	0	19/168
Mg(4)	6(*c*)	0	0	29/168
Mg(5)	6(*c*)	0	0	35/168
Mg(6)	6(*c*)	0	0	61/168
Mg(7)	6(*c*)	0	0	67/168
Zn,Ag(1)	3(*b*)	0	0	1/2
Zn,Ag(2)	6(*c*)	0	0	11/42
Zn,Ag(3)	6(*c*)	0	0	13/42
Zn,Ag(4)	6(*c*)	0	0	19/42
Zn,Ag(5)	9(*e*)	1/2	0	0
Zn,Ag(6)	18(*h*)	1/2	1/2	2/21
Zn,Ag(7)	18(*h*)	1/2	1/2	4/21
Zn,Ag(8)	18(*h*)	1/2	1/2	8/21

Table 2. *Comparison between the observed and calculated intensities of 02l reflexions for the two possible models of 6H structure*

h k l	Type 1 ($ABCA'C'B'$)	Type 2 ($ABC'B'AB'$)	I_o
0 2 0	0·0	6·7	weak
0 2 1	13·3	7·6	weak
0 2 2	54·3	10·3	weak
0 2 3	100·0	100·0	strong
0 2 4	92·9	17·7	weak
0 2 5	32·8	18·7	weak
0 2 6	0·0	16·0	weak
0 2 7	19·4	11·1	weak
0 2 8	31·6	6·0	weak
0 2 9	17·2	17·3	strong
0 2 10	4·3	0·8	weak
0 2 11	0·7	0·4	very weak
0 2 12	0·0	0·6	very weak

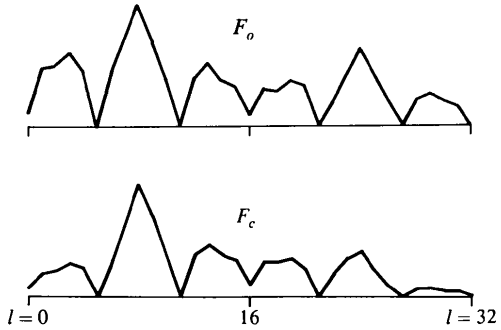

Fig. 4. Comparison of the observed (F_o) and calculated (F_c) structure factors of 02l reflexions for the best model of 16H.

stacking variants are so characteristic that their stacking sequences can be determined without any confusion.

There are only two possible models for the 6-layer type structure, *i.e.* (1) *ABCA'C'B'* and (2) *ABC'B'AB'*. The former is the structure already reported in the system $Mg(Ni_{1-x}Cu_x)_2$ (Komura, Nakaue & Mitarai, 1972) and $Mg(Ni_{1-x}Zn_x)_2$ (Komura, Mitarai, Nakaue & Tsujimoto, 1972). In making a comparison between visually observed intensities and those calculated we have concluded that the 6-layer structure is the latter model, *ABC'B'AB'*. Table 2 shows a list of calculated and observed intensities of 02l reflexions. The lattice parameters are $a = 5{\cdot}14$, $c = 25{\cdot}3$ Å, and the space group is $P\bar{6}m2$ with 12 formula units of $Mg(Cu_{0.535}Al_{0.465})_2$ in the unit cell.

A longer stacking variant, 16H, was also observed in the same alloy. From among more than 400 possible stacking models for the 16-layer type structure only one correct sequence was determined by referring to the characteristic features of the electron-diffraction pattern. The diffraction pattern shows that reflexions such as 0,k,5, 0,k,11, 0,k,21, 0,k,27 for $k = 1$ and 2 are barely recognised. The layer sequence thus determined can be expressed as *ABC'BCA'CAB'A'CA'C'BC'B'*. The agreement between calculated and observed structure factors is fairly good (Fig. 4). The new 16H structure has been concluded to be that of space group $P6_3/mmc$ with 32 formula units of $Mg(Cu_{0.535}Al_{0.465})_2$ in a unit cell with $a = 5{\cdot}14$, $c = 67{\cdot}4$ Å. The stacking sequences of these two structures were confirmed by the lattice images of the electron micrograph.

Stacking variants as a function of electron concentration

It was pointed out by Komura, Mitarai, Nakatini, Iba & Shimizu (1970), Komura, Nakaue & Mitarai (1972) and Komura, Mitarai, Nakaue & Tsujimoto (1972) that it is evident that the structural changes in the Mg-base ternary Friauf–Laves phases are a function of e/a, and the homogeneity ranges of the various stacking variants appear at nearly the same e/a values for all the

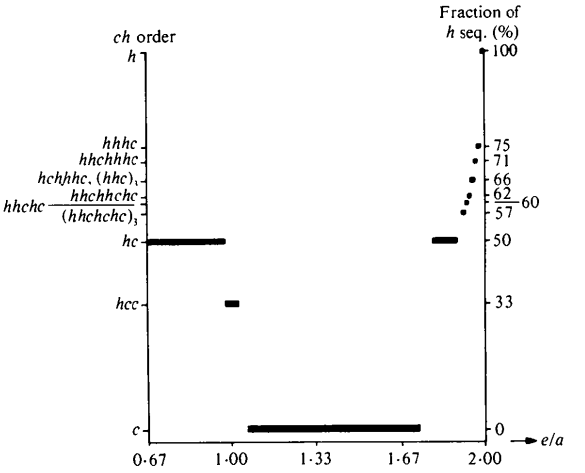

Fig. 5. Correspondence between the homogeneity range, the stacking sequence and the electron concentration for the Mg-base Friauf–Laves phases.

systems examined. The following structures were given in order of increasing e/a: 4-layer, 6-layer, 3-layer, 4-layer, 10-layer, 9-layer, 8-layer and 2-layer type structure. The fraction of the h sequence in these structures decreases with increasing e/a in the range 0·67–1·33, but increases with increasing e/a in the range 1·33–2·00. Approximate electron concentrations for the newly found stacking variants can be evaluated as 1·93 and 1·95, based on the nominal compositions $Mg(Zn_{0.90}Ag_{0.10})_2$ and $Mg(Cu_{0.535}Al_{0.465})_2$ respectively. Since the exact composition of such tiny single crystals cannot be known, let us locate these new structures at the proper positions in the series of stacking variants from the point of view of the fraction of the h sequence. Thus the electron concentration of the above structure comes out at a reasonable value expected for the nominal composition. In Table 3 is summarized the relation between electron concentration and the fraction of the h sequence of all the stacking variants together with the representation by Zhdanov symbol and *ch* order. The last column of the table shows the kinds of alloy systems. The homogeneity ranges of various stacking variants are presented in Fig. 5 where the fraction of the h sequence of the structure is plotted against electron concentration, and the *ch* order of the stacking variants is also shown on the left side. (The authors are grateful to Professor Parthé for showing us this type of presentation.) There is a remarkable correspondence between the homogeneity range, the stacking sequence and the electron concentration.

Discussion

Three new stacking variants of the rhombohedral 21-layer type, and hexagonal 6-layer and 16-layer types were found in the pseudobinary $MgZn_2$–$MgAg_2$ and

Table 3. *A list of stacking variants of* Mg-*base ternary Friauf–Laves phases*

e/a	Layer type	*ch* order	Zhdanov symbol	Fraction of *h* sequence (%)	Alloy
0·67 to 0·97	4*H*	$(hc)_2$	$2\bar{2}$	50	$MgNi_2$, Mg–Zn–Ni Mg–Cu–Ni
1·00	6*H*	$(hcc)_2$	$3\bar{3}$	33	Mg–Cu–Ni, Mg–Zn–Ni
1·07 to 1·73	3*C*	*ccc*	∞	0	$MgCu_2$, Mg–Zn–Ni Mg–Cu–Zn, Mg–Cu–Ni Mg–Zn–Ag, Mg–Zn–Li
1·80 to 1·89	4*H*	$(hc)_2$	$2\bar{2}$	50	Mg–Cu–Zn, Mg–Zn–Ni Mg–Zn–Ag, Mg–Zn–Li Mg–Cu–Al
1·93*	21*R*	$(hhchchc)_3$	$(2\bar{2}2\bar{1})_3$	57	Mg–Zn–Ag
1·93	10*H*	$(hhchc)_2$	$2\bar{1}2\bar{2}1\bar{2}$	60	Mg–Cu–Zn, Mg–Zn–Ni Mg–Zn–Ag, Mg–Zn–Li Mg–Cu–Al
1·95*	16*H*	$(hhchhchc)_2$	$2\bar{1}2\bar{1}2\bar{2}1\bar{2}1\bar{2}$	62	Mg–Cu–Al
1·95	9*R*	$(hhc)_3$	$(2\bar{1})_3$	66	Mg–Cu–Zn, Mg–Zn–Ni Mg–Zn–Ag, Mg–Zn–Li Mg–Cu–Al
1·95*	6*H*′	*hchhhc*	$2\bar{2}1\bar{1}$	66	Mg–Cu–Al
1·96	14*H*	$(hhchhhc)_2$	$2\bar{1}2\bar{1}1\bar{2}1\bar{2}1\bar{1}$	71	Mg–Zn–Li
1·98	8*H*	$(hhhc)_2$	$1\bar{2}1\bar{1}2\bar{1}$	75	Mg–Cu–Zn, Mg–Zn–Li Mg–Zn–Ag
2·00	2*H*	*hh*	$1\bar{1}$	100	$MgZn_2$, Mg–Zn–Li Mg–Cu–Al

* Nominal composition.

$MgCu_2$–$MgAl_2$ systems respectively. The crystal structures were analysed by single-crystal X-ray and electron-diffraction methods. The stacking sequences were then determined as *ABC′B′ABC′*BCA′*C′BCA′-CAB′A′CAB′*, *ABC′B′AB′* and *ABC′BCA′CAB′A′-CA′C′BC′B′* for 21*R*, 6*H* and 16*H*, their space groups being $R\bar{3}m$, $P\bar{6}m2$ and $P6_3/mmc$ respectively.

The intimate relation between the homogeneity range, the electron concentration and the stacking sequence, is recognised for many Mg-base alloy systems. The fractions of the *h* sequence for 21*R*, 6*H* and 16*H* structures are evaluated from the analysed layer stacking sequences. The three stacking variants, 21*R*, 6*H* and 16*H*, are thus located at proper positions in the series of increasing fraction of *h* sequence. No satisfactory explanation has been given so far on the relation between *e/a* and the stacking sequence, but the ideas of Blandin, Friedel & Saada (1966), Hodges (1967) and Havinga, van Vucht & Bushow (1969) must be helpful in interpreting the relation. Schubert (1974) presented an idea for the stacking variants of the Laves phase and he expected several stacking sequences as a function of *e/a*. However, the newly found 6*H* and 16*H* structures were not included in Table 1 in his paper.

The most striking feature for the sequence of these stacking variants is the fact that any stacking sequence represented by *ch* order does not contain more than two successive *c* sequences and four successive *h* sequences except for $C_{15}(MgCu_2)$, $C_{14}(MgZn_2)$ and *hcc* structures. This structural feature is very much different from those observed for other polytypic structures, such as SiC and ZnS, and this feature characterizes the stacking variants found in the Friauf–Laves phases. If we write the sequences in the Zhdanov symbols, the stacking sequences can be represented by the alternation of positive and negative changes of only 1 or 2. Interpretation of the lattice images of electron microscopy can be successfully made by utilizing this characteristic for the layer sequence.

There is an indication of other stacking variants existing in the region of $e/a \simeq 1{\cdot}90$, for example the 18*H* structure. Even though there are numerous possible stacking models, the number of plausible models for structure-factor calculation is very much limited by assuming the approximate fraction of *h* sequence from the nominal composition of the specimen. Thus, the analysis becomes much easier.

The appearance of so many stacking variants in the narrow region of *e/a* is somewhat puzzling. A coalescence of several stacking variants was sometimes observed even in a tiny specimen. This might be also due to a small concentration difference from one place to another in the specimen. Besides the electronic factor, there may be unknown factors governing the stabilization of the stacking variants in the Friauf–Laves phases. It is not known whether or not the same growth mechanism of polytypes observed in SiC and

ZnS is also operative for the present alloy systems. A study of crystal growth in the Friauf–Laves phase may be a key to solving the problem.

Diffuse streaks due to stacking faults are often observed in X-ray and electron-diffraction photographs. It is not known whether the kind of stacking fault derives from growth faults during crystallization or from deformation faults after growing the crystallites. However, even such a long-period stacking variant as 21*R* shows weak diffuse streaks, indicating that the phase is not metastable. The nature and analysis of the stacking faults will be discussed in a further publication.

The authors wish to express their gratitude to Mr Mitarai for his cooperation in part of this work. All the calculations were carried out on a TOSBAC-3400 computer at the Computing Center of Hiroshima University. The present work has been supported partly by a Scientific Research Grant from the Ministry of Education, to which the authors' thanks are due.

References

ALLEN, C. W., DELAVIGNETTE, P. & AMELINCKX, S. (1972). *Phys. Stat. Sol.* (*a*), **9**, 237–246.

BLANDIN, A., FRIEDEL, J. & SAADA, G. (1966). *J. Phys. Radium*, **27**, 128–136.

HAVINGA, E. E., VAN VUCHT, J. H. N. & BUSHOW, K. H. J. (1969). *Philips Res. Rep.* **24**, 407–426.

HODGES, C. H. (1967). *Acta Metall.* **15**, 1787–1794.

KITANO, Y., KOMURA, Y. & KAJIWARA, H. (1977). *Trans. Japan Inst. Met.* **18**, 39–45.

KOMURA, Y. (1962). *Acta Cryst.* **15**, 770–778.

KOMURA, Y., KISHIDA, E. & INOUE, M. (1967). *J. Phys. Soc. Japan*, **23**, 398–404.

KOMURA, Y., MITARAI, M., NAKATANI, I., IBA, H. & SHIMIZU, T. (1970). *Acta Cryst.* B**26**, 666–668.

KOMURA, Y., MITARAI, M., NAKAUE, A. & TSUJIMOTO, S. (1972). *Acta Cryst.* B**28**, 976–978.

KOMURA, Y., NAKAUE, A. & MITARAI, M. (1972). *Acta Cryst.* B**28**, 727–732.

KRIPYAKEVICH, P. I. & MELNYK, E. B. (1974). *Metallofiz. Kiev (USSR)*, **52**, 71–74.

LAVES, F. & WITTE, H. (1936). *Metallwirtschaft*, **15**, 840–842.

LIESER, K. H. & WITTE, H. (1952). *Z. Metallkd.* **43**, 396–401.

RAMSDELL, L. S. (1947). *Amer. Min.* **32**, 64–82.

SCHUBERT, K. (1974). *Acta Cryst.* B**30**, 1538–1540.

ZHDANOV, G. S. (1945). *C. R. Acad. Sci. URSS*, **48**, 40–43.

Acta Cryst. (1977). B**33**, 2501–2505

Conformation de Thio-Sucres Acycliques. III.* (Chloro-6 Purinyl-9)-1 Désoxy-1 Ethylthio-1 *aldéhydo*-D-Glucose Aldéhydrol

PAR ARNAUD DUCRUIX ET CLAUDINE PASCARD

Institut de Chimie des Substances Naturelles, CNRS, Laboratoire de Cristallochimie, 91190 *Gif/Yvette, France*

(*Reçu le* 24 *janvier* 1977, *accepté le* 7 *février* 1977)

The crystal structure of 1-(6-chloropurin-9-yl)-1-deoxy-1-ethylthio-*aldehydo*-D-glucose aldehydrol ($C_{12}H_{19}ClN_4O_5S$) has been determined by direct methods. The crystals are monoclinic, $a = 5{\cdot}537$, $b = 9{\cdot}010$, $c = 16{\cdot}848$ Å, $\beta = 94{\cdot}63°$, $Z = 2$ in space group $P2_1$. The intensities were collected on a four-circle diffractometer, with Mo $K\alpha$ radiation. The final R index is 0·06. The C chain of the sugar residue adopts a bent conformation with C(1) out of the plane defined by the other five C atoms. The configuration at the acetal C atom is (1*S*).

Introduction

Les observations faites par Horton & Wander (1969, 1974) sur les sucres acycliques ainsi que celles de Jeffrey & Kim (1970) sur les alditols à l'état cristallin ont montré que la conformation privilégiée d'un sucre acyclique est celle pour laquelle les atomes de carbone de la chaîne carbonée adoptent un arrangement plan, sauf si cette conformation est destabilisée par une ou plusieurs interactions parallèles éclipsées entre les substituants portés par des atomes de carbone en position alternée. Dans ce dernier cas, la molécule adopte une conformation plus stable en opérant une rotation de 120° autour d'une liaison C–C, ce qui conduit à une conformation dite 'repliée'.

Le dérivé étudié (I) se compose d'une chaîne acyclique et d'une base chloro-6 purine. Il est obtenu par condensation du chloro-6 (chloro-mercuri)-9 purine sur le dérivé monobromé et thioalkylé du D-glucose. La résolution de cette structure qui se situe dans le cadre

* Partie II: Ducruix & Pascard-Billy (1975*b*).